

# Supporting Information

## $[\text{P}_3\text{Se}_7]^{3-}$ : A Phosphorus-Rich Square-selenophosphate

In Chung,<sup>1</sup> Daniel Holmes,<sup>2</sup> David P. Weliky<sup>2</sup> and Mercuri G. Kanatzidis<sup>1\*</sup>

<sup>1</sup>*Department of Chemistry, Northwestern University, Evanston, IL 60208, USA*

<sup>2</sup>*Department of Chemistry, Michigan State University, East Lansing, MI 48824, USA*

\* To whom correspondence should be addressed:

Prof. Mercuri G. Kanatzidis

Department of Chemistry, Northwestern University, Evanston, IL 60208

m-kanatzidis@northwestern.edu

Tel) 847-467-1541

Fax) 847-491-5937

### Contents

#### Experimental Section

**Table S1.** Crystallographic Refinement Details for  $\text{Cs}_{10}\text{P}_8\text{Se}_{20}$ .

**Table S2.** Atomic coordinates ( $\times 10^4$ ) and equivalent isotropic displacement parameters ( $\text{\AA}^2 \times 10^3$ ) for  $\text{Cs}_{10}\text{P}_8\text{Se}_{20}$  at 100(2) K.

**Table S3.** Selected Bond Distances ( $\text{\AA}$ ) and Angles ( $^\circ$ ) for  $\text{Cs}_{10}\text{P}_8\text{Se}_{20}$  at 100(2) K.

**Figure S1.** Solid-state optical absorption spectrum of  $\text{Cs}_{10}\text{P}_8\text{Se}_{20}$ .

**Figure S2.** Raman spectrum of  $\text{Cs}_{10}\text{P}_8\text{Se}_{20}$ .

**Figure S3.** Far-IR spectrum of  $\text{Cs}_{10}\text{P}_8\text{Se}_{20}$ .

**Figure S4.** MAS  $^{31}\text{P}$  solid-state NMR spectrum of polycrystalline  $\text{Cs}_{10}\text{P}_8\text{Se}_{20}$ .

## Experimental Section

**X-ray Powder Diffraction.** X-ray powder diffraction analysis was performed using a calibrated CPS 120 INEL X-ray powder diffractometer (Cu  $K\alpha$  graphite monochromatized radiation) operating at 40 kV/20 mA and equipped with a position-sensitive detector with flat sample geometry.

**Scanning Electron Microscopy.** Semiquantitative analysis of the compound was obtained with a Hitachi S3400N-II scanning electron microscope (SEM) equipped with an ESED II detector.

**Solid-state UV-Vis spectroscopy.** Optical diffuse reflectance measurements were performed at room temperature using a Shimadzu UV-3101 PC double-beam, double-monochromator spectrophotometer operating in the 200-2500 nm region. The instrument is equipped with an integrating sphere and controlled by a personal computer. BaSO<sub>4</sub> was used as a 100% reflectance standard. The details are described elsewhere.<sup>1</sup>

**Raman Spectroscopy.** Raman spectrum was recorded on a Holoprobe Raman spectrograph equipped with a CCD camera detector using 633 nm radiation from a HeNe laser for excitation and a resolution of 4 cm<sup>-1</sup>. Laser power at the sample was estimated to be about 5 mW, and the focused laser beam diameter was ca. 10  $\mu$ m. A total of 128 scans was sufficient to obtain good quality spectra.

**Infrared Spectroscopy.** FT-IR spectrum was recorded as solids in a CsI matrix. The sample was ground with dry CsI into a fine powder and pressed into a translucent pellet. The spectra were recorded in the far-IR region (600-100 cm<sup>-1</sup>, 4 cm<sup>-1</sup> resolution) with the use of a Nicolet 740 FT-IR spectrometer equipped with a TGS/PE detector and silicon beam splitter.

**Differential Thermal Analysis (DTA).** Experiments were performed on a Shimadzu DTA-50 thermal analyzer. A sample (~30 mg) of ground crystalline material was sealed in a silica ampoule under vacuum. A similar ampoule of equal mass filled with Al<sub>2</sub>O<sub>3</sub> was sealed and placed on the reference side of the detector. The sample was heated to 550°C at a rate of 10°C min<sup>-1</sup>, and after 1 min it was cooled at -10°C min<sup>-1</sup> to 50 °C. The residue of the DTA experiments was examined by X-ray powder diffraction. Reproducibility of the results was confirmed by running multiple heating/cooling cycles. The melting and crystallization points were measured at onset of the endothermic peak and the exothermic peak.

**MAS <sup>31</sup>P NMR spectroscopy.** Bloch decay magic angle spinning <sup>31</sup>P NMR spectra of polycrystalline Cs<sub>10</sub>P<sub>8</sub>Se<sub>10</sub> were obtained at ambient temperature on a 9.4 T spectrometer (Varian Infinity Plus) using a 6 mm diameter rotor, spinning frequency of 5.0 or 6.0 kHz, <sup>31</sup>P frequency of 161.8 MHz, 15  $\mu$ s  $\pi/2$  pulse, and 1000 s recycle delay. Each spectrum was the sum of four scans and was referenced to phosphoric acid at 0 ppm. Each spectrum was processed with 50 Hz Gaussian line broadening and baseline correction.

**X-ray Crystallography.** Intensity data for Cs<sub>10</sub>P<sub>8</sub>Se<sub>20</sub> were collected at 100(2) K on a STOE IPDS 2T diffractometer with Mo  $K\alpha$  radiation operating at 50 kV and 30 mA with a 34 cm diameter imaging plate. Individual frames were collected with a 11 min exposure time and a 1.0  $\omega$  rotation. The X-Area, X-RED and X-SHAPE software package was used for data extraction and integration and to apply empirical and analytical absorption corrections (crystal dimension: 0.167  $\times$  0.118  $\times$  0.014 mm<sup>3</sup>). The SHELXTL software package was used to solve and refine the structure. The most satisfactory refinement was obtained with the centrosymmetric space group, *Pnmm*. All atoms were refined anisotropically. The Cs(4) atom was modeled as split into Cs(4A) and Cs(4B) sites. Their occupancy ratio was refined to 7:3. The site occupancy of the P(3) and P(4) atoms was refined to 25 %, respectively. All other atoms were refined to full occupancy. The parameters for data collection and the details of the structural refinement are given in Table S1. Fractional atomic coordinates and displacement parameters are given in Tables S2 and S3.

**Table S1.** Crystallographic Refinement Details for Cs<sub>10</sub>P<sub>8</sub>Se<sub>20</sub>.

Formula	Cs <sub>10</sub> P <sub>8</sub> Se <sub>20</sub>
Crystal system	Orthorhombic
Space group	<i>Pnmm</i> (no. 58)
Unit cell dimensions,	<i>a</i> = 26.5456(7) Å <i>b</i> = 8.0254(2) Å <i>c</i> = 11.9031(4) Å
<i>Z</i>	2
<i>V</i> , Å <sup>3</sup>	2535.8(1)
<i>d</i> (calculated), gr cm <sup>-3</sup>	4.133
Crystal dimensions, mm <sup>3</sup>	0.167 × 0.118 × 0.014
Temperature, K	100(2)
λ, Å	0.71073
μ, mm <sup>-1</sup>	21.711
F(000)	2700
θ <sub>max</sub> , deg	25.26
Total/unique reflections	15751/2242
<i>R</i> <sub>int</sub>	0.0555
No. Parameters	118
Refinement method	Full-matrix least-squares on F <sup>2</sup>
Final <i>R</i> indices [ <i>I</i> > 2σ( <i>I</i> )],	0.0339 / 0.0779
<i>R</i> <sub>1</sub> <sup>a</sup> / <i>wR</i> <sub>2</sub> <sup>b</sup>	
<i>R</i> indices (all data), <i>R</i> <sub>1</sub> / <i>wR</i> <sub>2</sub>	0.0391 / 0.0800
Goodness-of-fit on F <sup>2</sup>	1.159
Largest diff. peak and hole	0.793/-1.789 eÅ <sup>-3</sup>

$$^a R_1 = \frac{\sum ||F_o| - |F_c||}{\sum |F_o|}, \quad ^b wR_2 = \left\{ \frac{\sum [w(F_o^2 - F_c^2)^2]}{\sum [w(F_o^2)^2]} \right\}^{1/2}$$

**Table S2.** Atomic coordinates ( $\times 10^4$ ) and equivalent isotropic displacement parameters ( $\text{\AA}^2 \times$  $10^3$ ) for  $\text{Cs}_{10}\text{P}_8\text{Se}_{20}$  at 100(2) K.  $U_{eq}$  is defined as one third of the trace of the orthogonalized  $U_{ij}$  tensor.

	$x$	$y$	$z$	$U_{eq}$
Cs(1)	1986(1)	497(1)	0	29(1)
Cs(2)	611(1)	3197(1)	5000	32(1)
Cs(3)	0	0	2057(1)	44(1)
Cs(4A)	1349(2)	5567(3)	1991(1)	27(1)
Cs(4B)	1482(2)	5585(8)	2124(5)	27(1)
Se(1)	3316(1)	750(1)	0	30(1)
Se(2)	4365(1)	3668(2)	0	29(1)
Se(3)	3697(1)	6095(1)	2416(1)	31(1)
Se(4)	2592(1)	3416(1)	2416(1)	29(1)
Se(5)	2867(1)	6596(1)	0	31(1)
Se(6)	762(1)	2768(2)	0	29(1)
Se(7)	653(1)	7610(2)	0	38(1)
Se(8)	0	5000	2293(1)	45(1)
P(1)	4918(4)	2500	2978(3)	10(1)
P(2)	4927(1)	2500	7169(3)	11(1)
P(3)	7054(1)	2500	1014(1)	13(1)
P(4)	8481(1)	2500	7335(1)	15(1)

The occupancies of Cs(4A), Cs(4B), P(3) and P(4) are 70%, 30%, 25% and 25%, respectively. All other atoms are fully occupied.

**Table S3.** Selected Bond Distances (Å) and Angles (°) for Cs<sub>10</sub>P<sub>8</sub>Se<sub>20</sub> at 100(2) K.

P(1)-P(2)	2.294(3)	P(1)···P(4)	3.647(2)
P(3)-P(3)	2.264(16)	P(1)···P(5)	3.254(3)
P(4)-P(4)	2.237(16)	P(2)···P(2)	3.222(3)
P(1)-Se(1)	2.137(3)	P(3)···P(5)	3.645(1)
P(1)-Se(2)	2.132(3)		
P(2)-Se(3)	2.137(2)	P(2)-P(1)-P(2)	89.2(1)
P(2)-Se(4)	2.135(2)	P(1)-P(2)-Se(5)	90.31(9)
P(2)-Se(5)	2.295(2)	P(2)-Se(5)-P(2)	89.2(1)
P(3)-Se(6)	2.220(7)	Se(1)-P(1)-Se(2)	116.9(1)
P(3)-Se(7)	2.241(8)	Se(3)-P(2)-Se(4)	117.5(1)
P(3)-Se(8)	2.292(7)	Se(1)-P(1)-P(2)	111.7(1)
P(4)-Se(6)	2.257(8)	Se(2)-P(1)-P(2)	112.1(1)
P(4)-Se(7)	2.290(8)		
P(4)-Se(8)	2.267(8)		

**Figure S1.** Solid-state electronic optical absorption spectrum of  $\text{Cs}_{10}\text{P}_8\text{Se}_{20}$ .

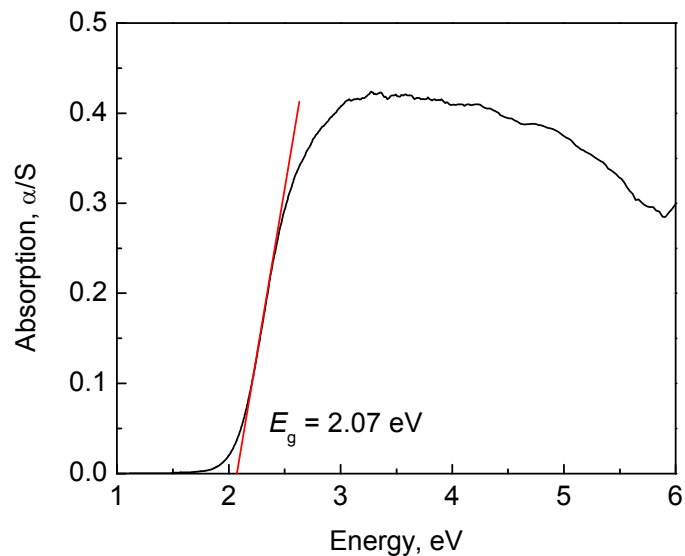


**Figure S2.** The Raman spectrum of  $\text{Cs}_{10}\text{P}_8\text{Se}_{20}$  shows shifts at 184(w), 214(vs), 254(w), 299(vw), 340(w), 351(w), 370(w), 457(w), 492(w), and 502(w)  $\text{cm}^{-1}$ . Peak positions are similar to those of selenophosphate cyclic molecules with low valent P such as  $\text{Rb}_4\text{P}_6\text{Se}_{12}$ ,<sup>2</sup>  $\text{Cs}_5\text{P}_5\text{Se}_{12}$ , and  $\text{Cs}_4\text{P}_6\text{Se}_{12}$ .<sup>3</sup>

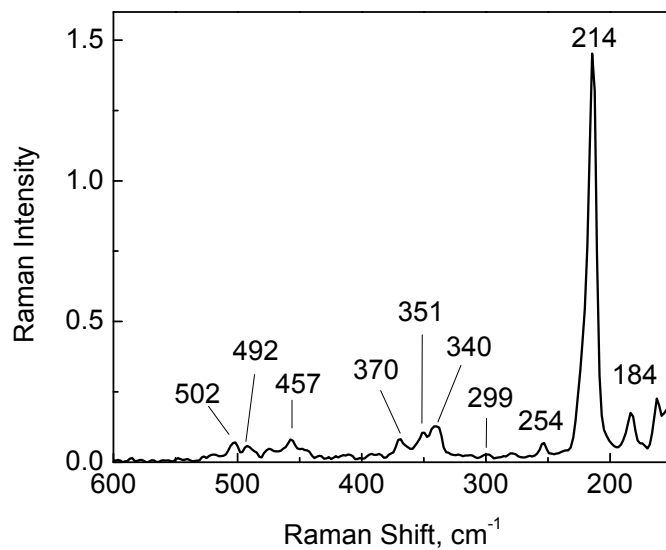


**Figure S3.** FT far-IR spectrum of  $\text{Cs}_{10}\text{P}_8\text{Se}_{20}$ .

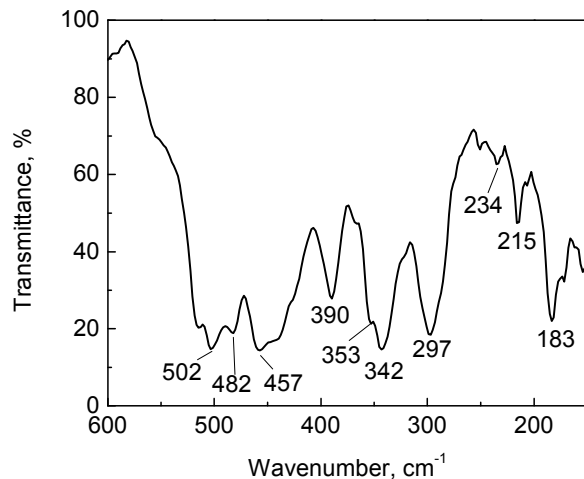
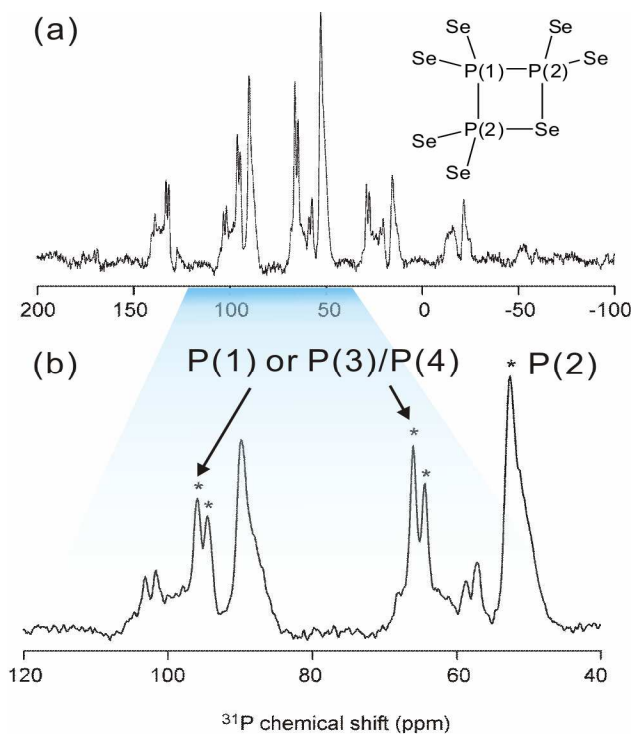


**Figure S4.** MAS  $^{31}\text{P}$  solid-state NMR spectrum of polycrystalline  $\text{Cs}_{10}\text{P}_8\text{Se}_{20}$  at 9.4 T field and 6.0 kHz spinning frequency. Panel (a) displays the full spectrum and panel (b) is an inset with the dominant isotropic peaks highlighted by asterisks. The  $[\text{P}_3\text{Se}_7]^{3-}$  anion is represented.



## References

- (1) Chung, I.; Song, J.-H.; Jang, I. J.; Freeman, A. J.; Ketterson, J. K.; Kanatzidis, G. *J. Am. Chem. Soc.* **2009**, *131*, 2647-2656, and references therein.
- (2) Chung, I.; Karst, A. L.; Weliky, D. P.; Kanatzidis, M. G. *Inorg. Chem.* **2006**, *45*, 2785.
- (3) Chung, I.; Jang, J. I.; Gave, M. A.; Weliky, D. P.; Kanatzidis, M. G. *Chem. Commun.* **2007**, 4998.